Available online at www.sciencedirect.com
ScienceDirect
Journal of the European Ceramic Society 29 (2009) 1795–1802
www.elsevier.com/locate/jeurceramsoc

Effects of CeO_2 addition on the properties of cordierite-bonded porous SiC ceramics

Shifeng Liu [a,b], Yu-ping Zeng [a,*], Dongliang Jiang [a]

[a] *Shanghai Institute of Ceramics, Chinese Academy of Science, 1295 Dingxi Road, Shanghai 20050, China*
[b] *Graduate School of the Chinese Academy of Science, Beijing 100049, China*

Received 6 June 2008; received in revised form 18 October 2008; accepted 4 November 2008
Available online 23 December 2008

Abstract

Cordierite-bonded porous SiC ceramics were fabricated with and without CeO_2 addition in air by an *in situ* reaction bonding technique. The effects of CeO_2 addition on the phase composition, microstructure and properties of porous SiC ceramics were investigated. It was found that the CeO_2 addition strongly promotes the phase transformation towards cordierite while inhibits the formation of spinel. With CeO_2 addition, the neck growth was enhanced, and the mechanical properties of porous SiC ceramics were improved. When 2.0 wt.% CeO_2 was added, a flexural strength of 35.3 MPa was achieved at an open porosity of 42.1%. Pore size distribution characterization by mercury porosimetry indicated that 2.0 wt.% CeO_2 addition enlarged the average pore size of porous SiC ceramics and introduced a bigger homogeneity in pore size. In addition, it was found that higher permeability was obtained after adding 2.0 wt.% CeO_2. Moreover, the thermal shock resistance of cordierite-bonded porous SiC ceramics was also improved by the addition of CeO_2.
© 2008 Elsevier Ltd. All rights reserved.

Keywords: Porous ceramics; Cordierite; SiC; CeO_2; Thermal shock resistance

1. Introduction

Porous ceramics attract increasing attention in the application for hot gas filtration in recent years.[1–6] For such application, the ceramic filters must be able not only to resist the chemical attack at high temperatures by the aggressive process environments containing steam, dust and gaseous sulfide, but also to withstand the mechanical strength decrease in the pulse-jet cleaning process. Due to the low thermal expansion coefficient, good thermal shock resistance, as well as excellent mechanical and chemical stability at elevated temperatures, porous SiC ceramics are thought to be the most promising filter material for hot gas filtration. However, it is hard to sinter SiC ceramics at moderate temperatures because of the strong covalent nature of Si–C bond.[7,8] A lot of works have been done to realize the fabrication of porous SiC ceramics at low temperature. She et al. developed an oxidation-bonding technique for the fabrication of porous SiC ceramics at low temperature.[9,10] In their works, SiC powder compacts were heated in air, SiC particles were then bonded by the oxidation-derived SiO_2 glass and the oxidation bonded porous SiC ceramics exhibit high fracture strength and good oxidation resistance. Furthermore, Ding et al. fabricated mullite-bonded porous SiC ceramics at 1450–1550 °C in air by an *in situ* reaction bonding technique.[11] Compared with the oxidation bonded porous SiC ceramics, the mullite-bonded porous SiC ceramics possess better high temperature stability and oxidation resistance.

Recently, we have fabricated cordierite ($2MgO{\cdot}2Al_2O_3{\cdot}5SiO_2$)-bonded porous SiC ceramics from SiC, Al_2O_3, MgO and graphite in air by the reaction bonding process at a relatively low temperature of 1350 °C.[12] The as-fabricated porous SiC ceramics possess high mechanical strength. In addition, the porous SiC ceramics are expected to exhibit good thermal shock resistance owing to the low thermal expansion coefficient of cordierite. Unfortunately, the cordierite phase is accompanied by the phase of spinel ($MgO{\cdot}Al_2O_3$), which impairs the thermal shock resistance of porous SiC ceramics due to the high thermal expansion coefficient of spinel. The positive influence of adding CeO_2 on promoting the phase transformation towards cordierite has been reported in the previous works.[13–17] Therefore, CeO_2 is

* Corresponding author. Tel.: +86 21 52415203; fax: +86 21 52413903.
E-mail address: yuping-zeng@mail.sic.ac.cn (Y.-p. Zeng).

0955-2219/$ – see front matter © 2008 Elsevier Ltd. All rights reserved.
doi:10.1016/j.jeurceramsoc.2008.11.002

chosen as the sintering additive in the present work to improve the properties of cordierite-bonded porous SiC ceramics. The effects of CeO_2 addition on the fabrication and properties of cordierite-bonded porous SiC ceramics were investigated.

2. Experimental procedure

Commercially available α-SiC powder (99.4% purity, 10.0 μm, Weifang Kaihua Silicon Carbide Micro-powder Co. Ltd., Weifang, China), α-Al_2O_3 (99.9% purity, 0.6 μm, Wusong Chemical Fertilizer Factory, Shanghai, China) and MgO (>98% purity, Shanghai Tongya Chemical Technology Co. Ltd., Shanghai, China) were used as the starting materials. Graphite powder (99.4% purity, 10.0 μm, Qingdao Huatai Lubricant Sealing Science and Technology Co. Ltd., Qingdao, China) was employed as the pore-forming agent. The weight ratio of SiC, Al_2O_3, MgO and graphite is 56.0:17.2:6.8:20.0, respectively (where the ratio of Al_2O_3 to MgO is equal to that in the stoichiometric composition of cordierite). CeO_2 (99.99% purity, Sinopharm Chemical Reagent Co. Ltd., Shanghai, China) was added into the mixture in nominal compositions as listed in Table 1. The powder mixtures were ball-milled in ethanol for 24 h to obtain homogeneous slurries, adding a small amount of PVB (polyvinyl butyral) as binder. After being dried in an oven at 80 °C and sieved through a 75-mesh (0.20 mm) screen, the mixed powders were bidirectionally pressed into the rectangular specimens with dimensions of ~5.0 mm × 10.0 mm × 50.0 mm under a 56 MPa pressure using a steel die. The specimens were sintered in air at 1150–1400 °C for 2 h with a heating and cooling rate of 5 °C/min.

All specimens were weighted before and after sintering to estimate the oxidation degree of SiC particles. Phase analysis was conducted by X-ray diffraction (XRD) (Model RAX-10, Rigaku, Japan) with Cu Kα radiation. Microstructures were observed by scanning electron microscopy (SEM) (Model JSM-5600LV, JEOL, Japan). Open porosity was determined by the Archimedes method with distilled water as the liquid medium. Pore size distribution was characterized by the mercury porosimetry (Model Pore-Sizer 9320, Micromeritics, USA). The gas permeability behaviour of porous SiC ceramics was evaluated by a home-made apparatus with nitrogen gas as a permeation medium. Flexural strength was measured via the three-point bending test (Model AUTO-GRAPH AG-1, Shimadzu, Japan) with a support distance of 30 mm and a cross-head speed of 0.5 mm/min, four specimens were tested to obtain the average strength and standard deviation. Thermal shock test was conducted by the conventional water-quenching technique.[18] The specimens were heated to the preset temperature at a rate of 5 °C/min and held for 0.5 h. Then, the specimens were quenched into a water bath, where the temperature was maintained at 20 °C. The residual strength of the specimens subjected to the water-quenching was determined at room temperature by the three-point bending test with a support distance of 30 mm and a cross-head speed of 0.5 mm/min.

Table 1
The weight percent of CeO_2 in the various specimens.

Specimen code	CeO_2 content (wt.%)
S0	0
S1	1.0
S2	2.0
S3	3.0
S4	4.0

3. Results and discussion

3.1. Effects of CeO_2 addition on the phase compositions of cordierite-bonded porous SiC ceramics

Fig. 1 shows the XRD patterns of the CeO_2-free specimens (S0) sintered at different temperatures. At 1200 °C, a large amount of metastable phase spinel forms as the result of the diffusive reaction between MgO and Al_2O_3 in solid state. Weak α-cordierite peaks appear at 1250 °C attributed to the dissolution of MgO and Al_2O_3 into SiO_2 and the subsequent turning into α-cordierite from the solid solution at its limit of solubility.[12] As the sintering temperature is increased to 1300 °C, more α-cordierite forms due to the higher temperature accelerates the solid diffusion. Above 1350 °C, the formation process of α-cordierite turns into crystallization directly from the liquid due to the liquid phase forms.[14] As a result, the formation of α-cordierite is further accelerated. On the other hand, the amount of spinel decreases gradually with the increase of the sintering temperature owing to the reaction between spinel and cristobalite.[19,20]

Fig. 2(a) and (b) shows the XRD patterns of the specimens with different CeO_2 contents sintered at 1200 and 1250 °C, respectively. CeO_2 addition strongly promotes the phase transformation towards α-cordierite. The α-cordierite peaks can be obviously observed in the XRD patterns of S1 to S4 at 1200 °C, and the α-cordierite peaks of S2 sintered at 1250 °C are even much more intensive than those of S0 sintered at 1350 °C. Moreover, it can be seen from Fig. 2 that the amount of α-cordierite increases continuously with the increase of the CeO_2 content. As expected, spinel phase decreases with the content of CeO_2. Only a trace of spinel was detected in the XRD pat-

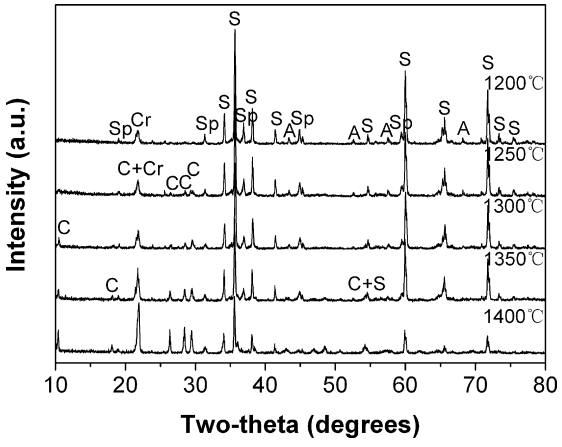

Fig. 1. XRD patterns of S0 sintered at different temperatures (S is SiC, C is α-cordierite, A is α-Al_2O_3, Cr is cristobalite and Sp is spinel).

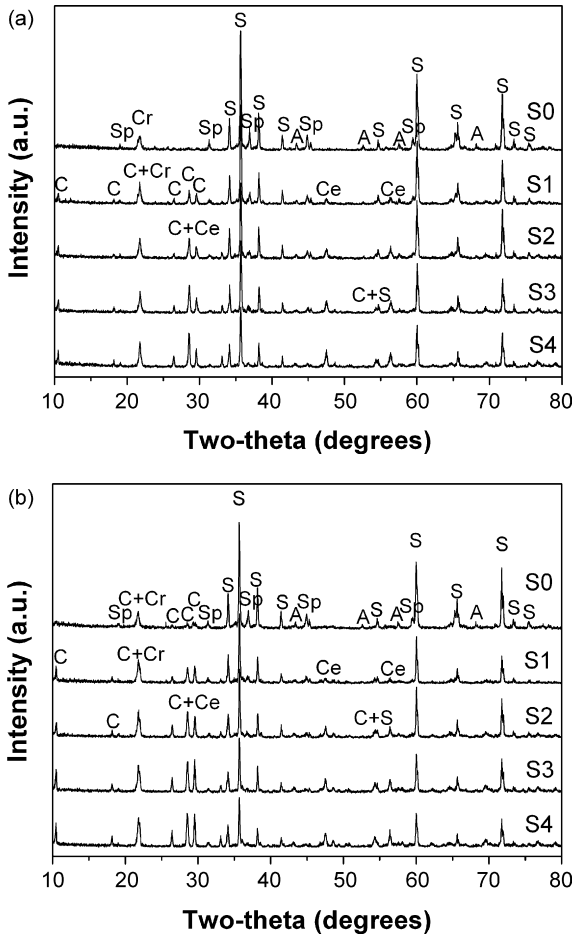

Fig. 2. XRD patterns of the specimens with different CeO_2 contents sintered at (a) 1200 °C and (b) 1250 °C (S is SiC, C is α-cordierite, A is α-Al_2O_3, Cr is cristobalite, Sp is spinel and Ce is CeO_2).

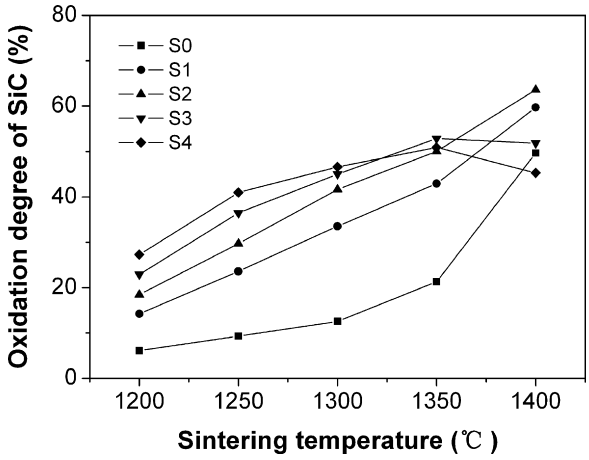

Fig. 3. Plots of oxidation degree of SiC vs. sintering temperature for the specimens with different CeO_2 contents.

terns of S2 to S4 sintered at 1250 °C. These observations are well in agreement with the results reported by Shi et al. about the effects of CeO_2 on phase transformation towards cordierite in MgO–Al_2O_3–SiO_2 system.[14,17] Based on their works,[14,17] Ce^{4+} can weaken the bonds of Mg–O and Al–O by attaching O^{2-} from MgO and Al_2O_3 crystals. As a result, the addition of CeO_2 inhibits the combination of MgO and Al_2O_3 into spinel while promotes the dissolution of MgO and Al_2O_3 into cristobalite and so, accelerates the reaction to form α-cordierite. In the present work, the enhancement of phase transformation towards cordierite at 1200–1250 °C by the addition of CeO_2 can be associated with the alteration of solid ion diffusion. In addition, it is worth noting that a proper amount of CeO_2 addition can not only lower the formation temperature of liquid to about 1280 °C in MgO–Al_2O_3–SiO_2 system, but also make ionic diffusion easier in liquid.[14] Therefore, CeO_2 addition can also facilitate cordierite crystallization.

According to the work by Montanaro,[21] the solid solubility of Ce^{4+} in cordierite is very low. Moreover, there is no reaction between CeO_2 and cordierite. Fig. 2 proves that Ce^{4+} is mainly existed in the forms of CeO_2 at 1200–1250 °C. It can be seen from Fig. 2 that the obvious CeO_2 peaks exist in the XRD patterns of S2 to S4.

CeO_2 addition also promotes the oxidation of SiC. Fig. 3 shows the plots of oxidation degree of SiC vs. sintering temperature for the specimens with different CeO_2 contents. Both the elevation of sintering temperature and the addition of CeO_2 promote the oxidation of SiC at 1200–1350 °C. Based on previous works,[22,23] the oxidation-derived silica forms a protective film and the rate of oxidation is diffusion controlled. It is generally accepted that the mobile species is oxygen, not silicon. The transport of oxygen through SiO_2 can occur by diffusion of molecular oxygen as interstitials or by network exchange of ionic oxygen.[24–26] According to the work by Costello and Tressler,[25] the activation energy for oxidation of SiC is low (120 kJ/mol) below 1400 °C, and is similar to that for oxidation of pure silicon and molecular oxygen diffusion through amorphous SiO_2, which indicated that oxidation in this temperature regime is controlled by the permeation of molecular oxygen through the growing oxide film. Considering the relatively low sintering temperatures in the present work, molecular oxygen diffusion inward should be the rate-controlling step for the oxidation of SiC. Molecular oxygen diffusion through silica film becomes faster at higher temperature and so, the oxidation of SiC is speeded up. On the other hand, CeO_2 addition may also promote the oxidation of SiC owing to the fact that the CeO_2 addition accelerates the dissolution of MgO and Al_2O_3 into SiO_2. However, it is interesting to find that the specimen with a high CeO_2 addition (S4) exhibits a slightly lower SiC oxidation degree than CeO_2-free specimen (S0) at 1400 °C. It is known CeO_2 addition can decrease the viscosity of liquid and facilitate densification and cordierite crystallization in MgO–Al_2O_3–SiO_2 system.[27] So, a high CeO_2 addition may cause a rapid densification to occur in the region near the surface of the specimen at a relatively high temperature (1400 °C), which inhibits the inward diffusion of oxygen. As a result, too much CeO_2 addition induces a decrease of SiC oxidation degree at a relatively high temperature.

It is noteworthy that proper CeO_2 addition reduces the amount of cristobalite in the cordierite-bonded porous SiC ceramics due to the promotion of the phase transformation towards cordierite. As shown in Figs. 1 and 2(b), the XRD pattern of S2 sintered at

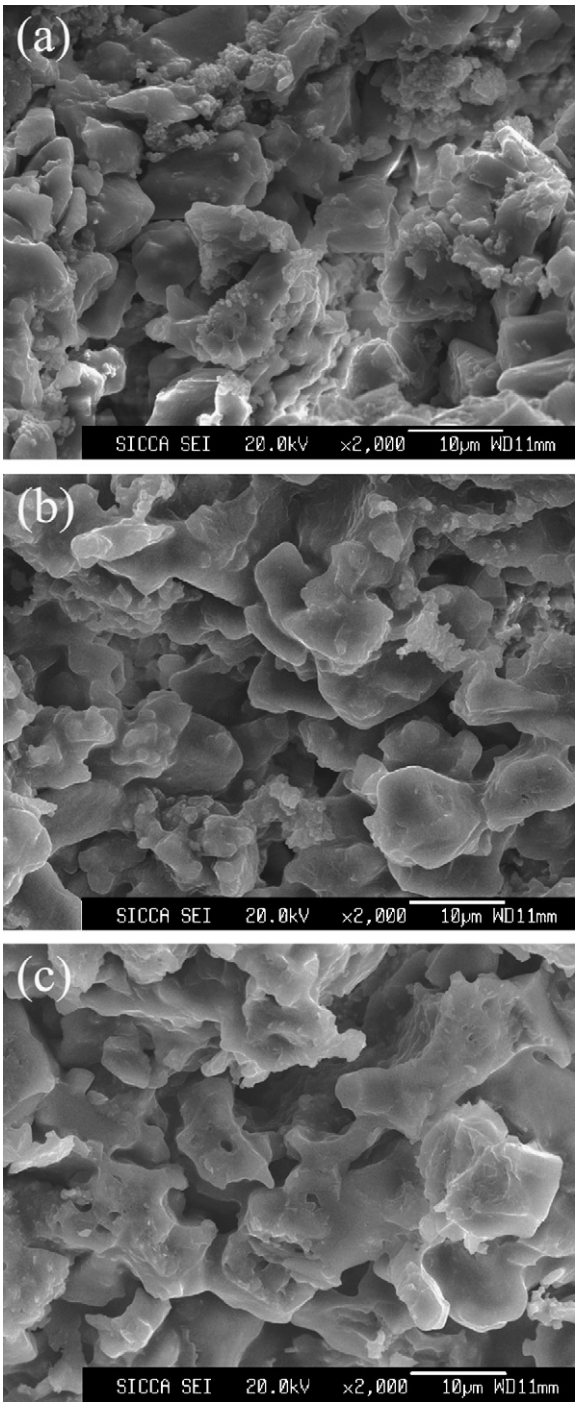

Fig. 4. SEM micrographs of fracture surfaces of (a) S0 sintered at 1250 °C, (b) S0 sintered at 1350 °C and (c) S2 sintered at 1250 °C.

1250 °C exhibits more intensive α-cordierite peaks while weaker cristobalite peaks than that of S0 sintered at 1350 °C.

3.2. Effects of CeO_2 addition on the microstructure of cordierite-bonded porous SiC ceramics

Fig. 4(a) shows the typical microstructures of S0 sintered at 1250 °C. The SEM micrograph exhibits a loose structure with connected pores. In addition, there are many agglomerates on

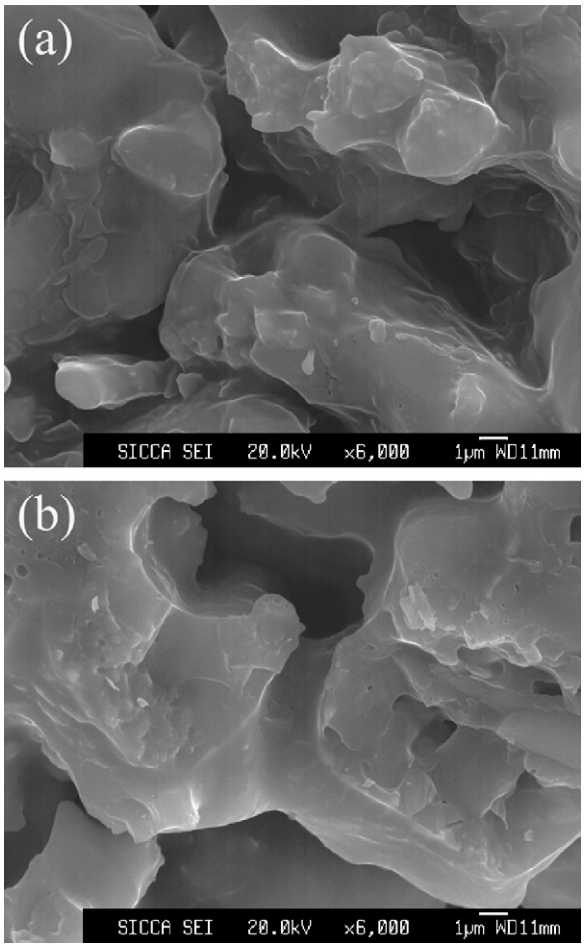

Fig. 5. Typical bonding necks in (a) S0 sintered at 1350 °C and (b) S2 sintered at 1250 °C.

the surface of SiC particles, which are mainly the unreacted alumina based on the XRD results in Fig. 1. When the sintering temperature is increased to 1350 °C, the well-developed bonding necks are formed between SiC particles in S0 as shown in Fig. 4(b). This should be attributed to the formation of a large amount of cordierite. Fig. 4(c) shows the typical microstructure of S2 sintered at 1250 °C. The SEM micrograph of S2 exhibits a microstructure with compacted bonding between SiC particles. Fig. 5 indicates that the bonding necks of S2 sintered at 1250 °C are even much thicker than those of S0 sintered at 1350 °C. This reason is that there is much more cordierite in S2 sintered at 1250 °C than that of S0 sintered at 1350 °C.

It is worth noting that there are two types of pores with different pore sizes in S0 sintered at 1250 or 1350 °C, as shown in Fig. 4(a) and (b). Due to 10.0 μm SiC and 10.0 μm graphite particles were used as the starting materials, the small pores are derived from stacking of SiC particles while the big pores are caused by graphite burnout. On the other hand, it can be seen from Fig. 4(c) that the pores derived from stacking of SiC particles almost disappear in S2 after sintered at 1250 °C. The pore size distribution of S0 sintered at 1350 °C and S2 sintered at 1250 °C are agreement with the above SEM results very well. As shown in Fig. 6, S0 sintered at 1350 °C exhibits bimodal pore size distribution, while S2 sintered at 1250 °C shows unimodal

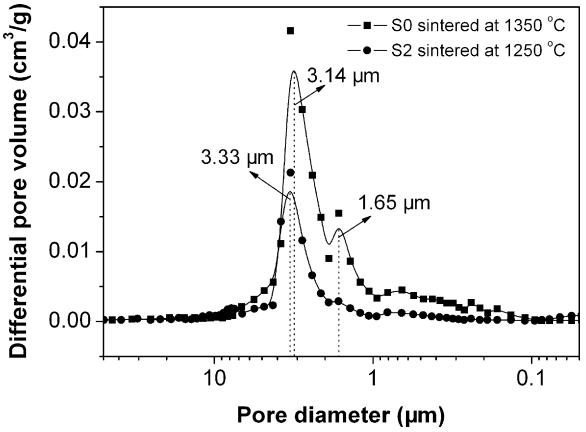

Fig. 6. Pore size distribution in S0 sintered at 1350 °C and S2 sintered at 1250 °C.

pore size distribution. It is often observed that small pores are tended to be merged into big pores as sintering proceeds. With CeO_2 addition, ion diffusion is accelerated, which promotes the sintering process. As a result, the small pores almost disappear in S2 after sintering at 1250 °C. Evidently, the bigger homogeneity in pore size after CeO_2 addition is in favor of particulate filtration efficiency in the application for hot gas filtration. Moreover, S2 sintered at 1250 °C possesses higher permeability than S0 sintered at 1350 °C, though the open porosity of S2 sintered at 1250 °C (42.1%) is lower than that of S0 sintered at 1350 °C (49.6%). The permeability of porous SiC ceramics was evaluated using Forchheimer's equation for the compressible gas as follows[28,29]:

$$\frac{P_i^2 - P_o^2}{2PL} = \frac{\eta}{K_1} V_s + \frac{\rho}{K_2} V_s^2 \quad (1)$$

where P_i is the fluid pressure at the entrance of the sample, P_o is the fluid pressure at the exit of the sample, V_s is the fluid velocity, P is the fluid pressure at which V_s is measured, L is the sample thickness, η is the viscosity of the fluid, ρ is the density of the fluid, K_1 is the Darcian or viscous permeability and K_2 is the non-Darcian or inertial permeability. The first term ($\eta V_s/K_1$) represents viscous energy losses, while the second term ($\rho V_s^2/K_2$) represents inertia energy losses. The fit of this equation to the results in Fig. 7 gave $\eta/K_1 = 250.7\ (\text{MPa s})/\text{m}^2$ and $\rho/K_2 = 77.57\ (\text{MPa s}^2)/\text{m}^3$, with a correlation factor $R^2 = 0.99997$ for S0 sintered at 1350 °C, while gave $\eta/K_1 = 203.1\ (\text{MPa s})/\text{m}^2$ and $\rho/K_2 = 51.75\ (\text{MPa s}^2)/\text{m}^3$, with a correlation factor $R^2 = 0.99999$ for S2 sintered at 1250 °C. Such high R^2 values indicate that the permeability of porous SiC ceramics can be well evaluated by Eq. (1). Darcian permeability K_1 and non-Darcian permeability K_2 can be calculated from the values of η/K_1 and ρ/K_2 (at room temperature, viscosity η and density ρ of N_2 are 1.78×10^{-5} Pa s and $1.16\ \text{kg/m}^3$, respectively). It is obtained that K_1 and K_2 of S2 sintered at 1250 °C ($0.710 \times 10^{-13}\ \text{m}^2$ and 0.0150×10^{-6} m, respectively) were both higher than those of S0 sintered at 1350 °C ($0.876 \times 10^{-13}\ \text{m}^2$ and 0.0224×10^{-6} m, respectively). The Darcian permeability K_1 of porous ceramics can be estimated

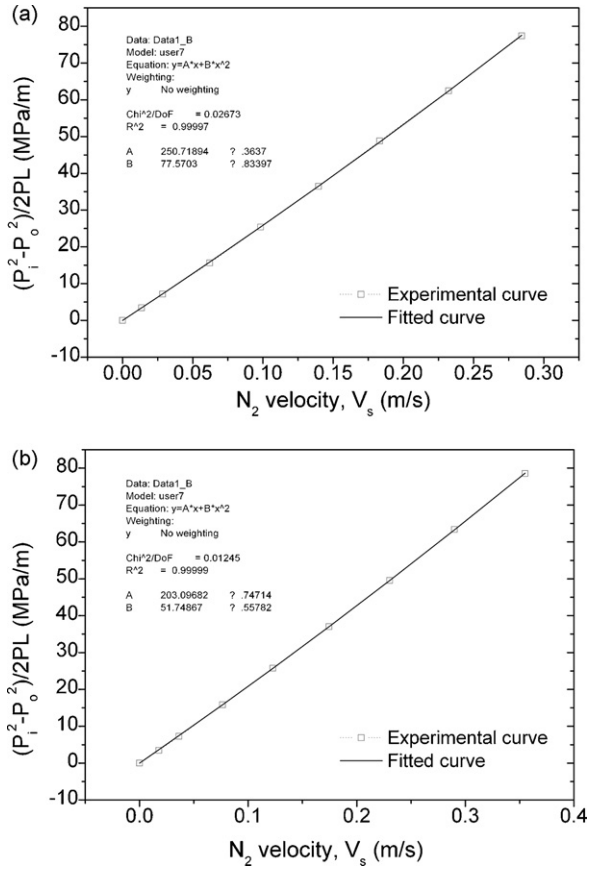

Fig. 7. Relationship between pressure gradient and N_2 velocity for (a) S0 sintered at 1350 °C and (b) S2 sintered at 1250 °C, where experimental data are fitted to Eq. (1).

by the Carman–Kozeny's relation[30]:

$$K_1 = \frac{pd^2}{16 f_{CK} \tau^2} \quad (2)$$

where p is the efficient porosity contributing to the permeability, d is the average pore diameter, f_{CK} is Carman–Kozeny coefficient, and τ is the tortuosity of pore channels. Based on the results of investigation on pore size distribution, the average pore diameter of S0 sintered at 1350 °C and S2 sintered at 1250 °C are 2.42 and 3.16 μm, respectively. According to Eq. (2), it is not surprise that S2 sintered at 1250 °C exhibits a high Darcian permeability than S0 sintered at 1350 °C though the open porosity of S2 sintered at 1250 °C is slightly lower than that of S0 sintered at 1350 °C. On the other hand, the bigger homogeneity in pore size after CeO_2 addition causes less tortuous flow paths to be generated. Then, the inertia interaction between gas and porous walls is weakened. Therefore, S2 sintered at 1250 °C also exhibits a high non-Darcian permeability than S0 sintered at 1350 °C.

3.3. Effects of CeO_2 addition on the properties of cordierite-bonded porous SiC ceramics

Fig. 8 shows the plots of open porosity vs. sintering temperature for the specimens with different CeO_2 contents. Open porosity decreases with sintering temperature for all specimens.

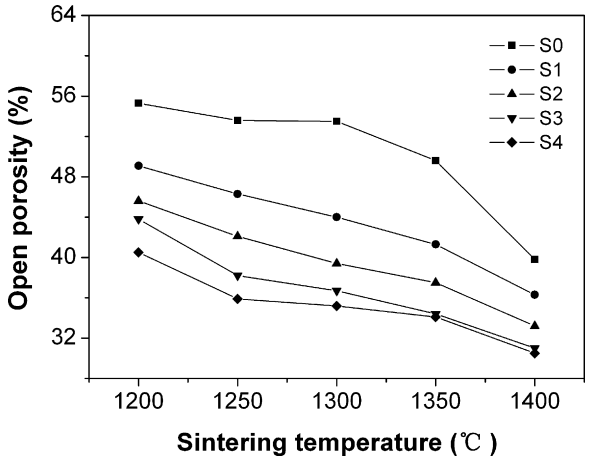

Fig. 8. Plots of open porosity vs. sintering temperature for porous SiC ceramics with different CeO_2 contents.

In addition, open porosity of the porous SiC ceramics with CeO_2 addition (S1 to S4) is smaller than the one without CeO_2 addition. According to the theoretic calculation, the oxidation of SiC to cristobalite is accompanied with acute volume expansion (108%). Part of this expanded volume will be extended into the voids among SiC particles and leads to the decrease of open porosity. In addition, the sintering densification also leads to the decrease of open porosity. In the sintering temperature range of 1200–1350 °C, both the increase of the sintering temperature and the addition of CeO_2 promote the oxidation of SiC and the sintering densification behaviour, resulting in the decreases of the open porosity. At a relatively high temperature of 1400 °C, specimen with a high CeO_2 addition (S4) exhibits a slightly lower SiC oxidation degree than CeO_2-free specimen (S0), however, the open porosity of S4 was much lower than that of S0. This should be attributed to the fact the sintering densification behaviour was strongly promoted by the CeO_2 addition when the sintering temperature was relatively high.

Fig. 9 shows the flexural strength of porous ceramics as a function of sintering temperature for the specimens with different CeO_2 contents. When the sintering temperature is 1200 °C, the flexural strength is notably improved by the addition of CeO_2

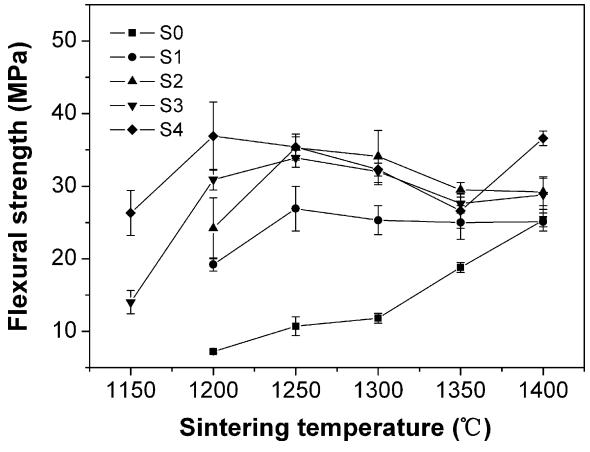

Fig. 9. Plots of flexural strength vs. sintering temperature for porous SiC ceramics with different CeO_2 contents.

and S4 exhibits the highest flexural strength of 36.9 MPa. As the sintering temperature is increased to 1250 °C, the flexural strength is improved for S0 to S3, but is impaired for S4. The flexural strength of S2 is 35.3 MPa, which is almost equal to that of S4 (35.4 MPa). At 1300 and 1350 °C, the flexural strength shows a decrease for all specimens except S0. As the sintering temperature is further increased to 1400 °C, the flexural strength of S0, S3 and S4 increases, while the flexural strength of S1 and S2 almost has not changed.

The mechanical strength of porous ceramics depends strongly on porosity. The strength–porosity dependence can be approximated as follows[31,32]:

$$\sigma = \sigma_0 \exp(-bp) \tag{3}$$

where σ is the strength of the porous structure at a porosity p, σ_0 is the strength of a nonporous structure and b is an empirical constant that is dependent on the pore characteristics. From the literature,[9] the closed porosity of OBSCs was very less (about 0.3–0.4%). Thus, the closed porosity of porous SiC ceramics in the present work can be neglected. It can be seen from Fig. 9 that the flexural strength was notably improved by CeO_2 addition at 1200–1250 °C. Obviously, the decrease of porosity with CeO_2 addition has contribution to the improvement of the flexural strength. Moreover, CeO_2 addition promotes the phase transformation towards cordierite, which induces the enhancement of neck growth and improves the flexural strength. However, the flexural strength of S2 to S4 exhibits obvious decreases at 1300 and 1350 °C, though their porosities decrease. This should be attributed to the high SiC oxidation degree of these specimens at 1300 and 1350 °C, which causes much cristobalite to be existed in the specimens and impairs the flexural strength of porous SiC ceramics. With the temperature increases to 1400 °C, the SiC oxidation degree and porosity of S4 both decrease. As a result, the flexural strength of S4 increases sharply.

Combining the results in Figs. 8 and 9, it is obvious that S2 sintered at 1250 °C exhibits better mechanical properties than S0 sintered at 1400 °C. The flexural strength and open porosity of S2 sintered at 1250 °C (35.3 MPa and 42.1%, respectively) were both higher than those of S0 sintered at 1400 °C (25.3 MPa and 39.8%, respectively). However, it cannot be identified if the higher flexural strength of S2 sintered at 1250 °C relative to S0 sintered at 1350 °C is not due only to the lower porosity. To achieve a better understanding of the effect of CeO_2 addition on the mechanical properties of cordierite-bonded porous SiC ceramics, plots of flexural strength vs. porosity for the specimens without and with CeO_2 addition were compared. Porosity was changed by varying the amount of graphite addition. For the specimens with CeO_2 addition, the weight ratio of CeO_2 to $SiC + MgO + Al_2O_3$ was fixed to the value of 0.0255 in the starting materials, which is equal to the weight ratio of CeO_2 to $SiC + MgO + Al_2O_3$ in S2. The specimens without and with CeO_2 addition were sintered at 1350 and 1250 °C for 2 h, respectively. The plots of flexural strength vs. porosity for the specimens without and with CeO_2 addition were constructed as shown in Fig. 10. The fit of Eq. (3) to the results in Fig. 10

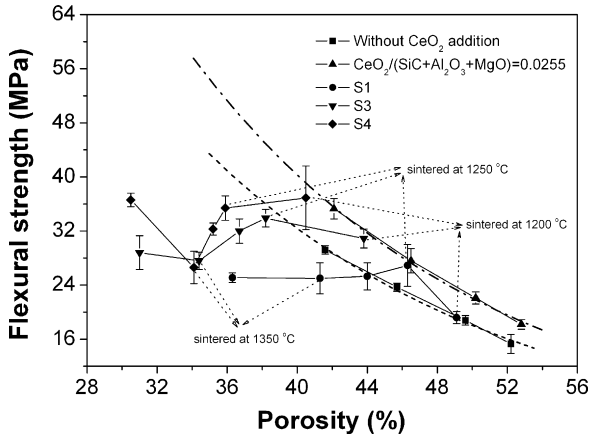

Fig. 10. Flexural strength as a function of porosity for the porous SiC ceramics without and with CeO_2 addition. Specimens without CeO_2 addition and with $CeO_2/(SiC + MgO + Al_2O_3) = 0.0255$ were sintered at 1350 and 1250 °C, respectively. S1, S3 and S4 were sintered at 1200–1400 °C.

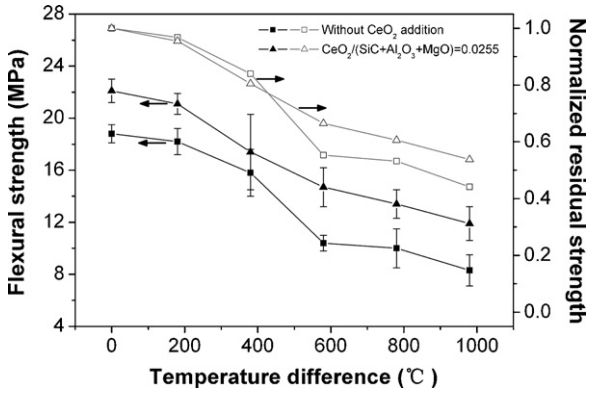

Fig. 11. Residual flexural strength and normalized residual strength as a function of quenching temperature difference for the specimens without and with CeO_2 addition.

shows that the flexural strength of the specimen with CeO_2 addition was higher than that of the specimen without CeO_2 addition at a same porosity. This indicates that CeO_2 addition has a good effect on the mechanical properties of cordierite-bonded porous SiC ceramics. As mentioned earlier, CeO_2 addition enhances the growth of the necks among SiC particles. According to the work by Rice,[31,33] the fracture strength of porous ceramics is determined by the actual load-bearing area or the minimum solid area. Therefore, the strength of porous SiC ceramics was improved by the enhancement of the neck growth. Relationships between flexural strength and porosity of S1, S3 and S4 sintered at 1200–1400 °C were also shown in Fig. 10. It is noteworthy that the exponential relationship between strength and porosity is not applicable to these specimens which sintered at different temperatures. This is due to the fact that the phase compositions of specimens are changed with sintering temperature, which strongly affects the strength of the specimens. It can be seen from Fig. 10 that all points except S1 sintered at 1250 °C, S3 sintered at 1200 °C and S4 sintered at 1200 °C were in the region beneath the fitted curve of CeO_2-free specimen sintered at 1350 °C, while these three points were in the region above the fitted curve of CeO_2-free specimen sintered at 1350 °C but beneath the fitted curve of the specimen with $CeO_2/(SiC + MgO + Al_2O_3) = 0.0255$ sintered at 1250 °C. These results indicate that proper amount of CeO_2 addition aids in improving the mechanical properties of cordierite-bonded porous SiC ceramics.

CeO_2-free specimen sintered at 1350 °C and CeO_2-added specimen (the weight ratio of CeO_2 to $SiC + MgO + Al_2O_3$ is 0.0255) sintered at 1250 °C with nearly same open porosities (49.6% and 50.2%, respectively) were selected to investigate the effect of the CeO_2 addition on the thermal shock resistance of porous SiC ceramics. Fig. 11 shows the residual strength of the quenched specimens as a function of quenching temperature difference. Both specimens did not show an abrupt strength decrease, but exhibited a gradual strength reduction. The same phenomena were previously observed in the oxidation bonded porous SiC ceramics and mullite-bonded porous SiC ceramics.[34,35] It is known that the bulk temperature gradient may give rise to a maximum tensile stress in the surface of the quenched specimens.[36] Some weak necks in the surface region would be cracked during the quenching temperature. However, the crack propagation is difficult in porous ceramics due to the crack–pore interactions.[34] Thus, the residual strength only decreases gradually with the increase of quenching temperature difference.

As expected, CeO_2 addition improves the thermal shock resistance of cordierite-bonded porous SiC ceramics. Fig. 11 shows that the residual flexural strengths of CeO_2-added specimen were higher than those of CeO_2-free specimen at all temperature differences. Moreover, the effect of CeO_2 addition on the normalized residual strength for various thermal shock temperature differences is shown in Fig. 11. The residual flexural strength values of the specimens after thermal shock are normalized with those before thermal shock. As can be seen, the thermal shock resistance of cordierite-bonded porous SiC ceramics was improved by CeO_2 addition. This should be attributed to the effect of CeO_2 addition on the phase compositions of cordierite-bonded porous SiC ceramics. CeO_2 addition promotes the phase transformation towards cordierite, while inhibits the formation of spinel and reduces the amount of residual cristobalite, which effectively lowers the thermal expansion coefficient of porous SiC ceramics. Hence, the thermal shock resistance of cordierite-bonded porous SiC ceramics is improved by the addition of CeO_2.

4. Conclusions

Cordierite-bonded porous SiC ceramics were fabricated with and without CeO_2 addition from SiC, α-Al_2O_3, MgO and graphite in air by the *in situ* reaction bonding process. CeO_2 addition strongly promotes the phase transformation towards cordierite, while inhibits the formation of spinel. When 2.0 wt.% CeO_2 was added, a large amount of cordierite but only a trace of spinel was formed at 1250 °C. Due to the enhancement of neck growth by the addition of CeO_2, porous SiC ceramics with CeO_2 addition exhibit better mechanical properties than the one without CeO_2 addition. When 2.0 wt.% CeO_2 was added, a high

flexural strength of 35.3 MPa is achieved at an open porosity of 42.1%. In addition, it was found that the addition of 2.0 wt.% CeO_2 introduced a bigger homogeneity in pore size and enlarged the average pore size of porous SiC ceramics. In the meantime, higher permeability was obtained after adding 2.0 wt.% CeO_2. Moreover, CeO_2 addition improves the thermal shock resistance of cordierite-bonded porous SiC ceramics.

Acknowledgement

The authors would like to thank the "Plan of Outstanding Talents" of Chinese Academy of Science and the Shanghai of Committee Science and Technology under the object "07jp14093" for the financial support.

References

1. Pastila, P. H., Helanti, V., Nikkila, A. P. and Mantyla, T. A., Effect of crystallization on creep of clay bonded SiC filters. *Ceram. Eng. Sci. Proc.*, 1998, **19**(4), 37–44.
2. Alvin, M. A., Impact of char and ash fines on porous ceramic filter life. *Fuel Process. Technol.*, 1998, **56**(1–2), 143–168.
3. Pastila, P., Helanti, V., Nikkila, A. P. and Mantyla, T., Environmental effects on microstructure and strength of SiC-based hot gas filters. *J. Eur. Ceram. Soc.*, 2001, **21**(9), 1261–1268.
4. Kanaoka, C. and Amornkitbamrung, M., Effect of filter permeability on the release of captured dust from a rigid ceramic filter surface. *Powder Technol.*, 2001, **118**(1–2), 113–120.
5. Heidenreich, S. and Scheibner, B., Hot gas filtration with ceramic filters: experiences and new developments. *Filtr. Separat.*, 2002, **39**(4), 22–25.
6. Heidenreich, S. and Wolters, C., Hot gas filter contributes to IGCC power plant's reliable operation. *Filtr. Separat.*, 2004, **41**(5), 22–24.
7. Riedel, R., Passing, G., Schonfelder, H. and Brook, R. J., Synthesis of dense silicon-based ceramics at low temperatures. *Nature*, 1992, **355**(6362), 714–717.
8. Sigl, L. S. and Kleebe, H. J., Core/rim structure of liquid-phase-sintered silicon carbide. *J. Am. Ceram. Soc.*, 1993, **76**(3), 773–776.
9. She, J. H., Yang, J. F., Kondo, N., Ohji, T., Kanzaki, S. and Deng, Z. Y., High-strength porous silicon carbide ceramics by an oxidation-bonding technique. *J. Am. Ceram. Soc.*, 2002, **85**(11), 2852–2854.
10. She, J. H., Ohji, T. and Kanzaki, S., Oxidation bonding of porous silicon carbide ceramics with synergistic performance. *J. Eur. Ceram. Soc.*, 2004, **24**(2), 331–334.
11. Ding, S. Q., Zhu, S. M., Zeng, Y. P. and Jiang, D. L., Fabrication of mullite-bonded porous silicon carbide ceramics by *in situ* reaction bonding. *J. Eur. Ceram. Soc.*, 2007, **27**(4), 2095–2102.
12. Liu, S. F., Zeng, Y. P. and Jiang, D. L., Fabrication and characterization of cordierite-bonded porous SiC ceramics. *Ceram. Int.*, 2009, **35**, 597–602.
13. Kim, B. H. and Lee, K. H., Crystallization and sinterability of cordierite-based glass powders containing CeO_2. *J. Mater. Sci.*, 1994, **29**(24), 6592–6598.
14. Shi, Z. M., Liang, K. M. and Gu, S. R., Effects of CeO_2 on phase transformation towards cordierite in $MgO–Al_2O_3–SiO_2$ system. *Mater. Lett.*, 2001, **51**(1), 68–72.
15. Shi, Z. M., Liang, K. M., Zhang, Q. and Gu, S. R., Effects of cerium addition on phase transformation and microstructure of cordierite ceramics prepared by sol–gel method. *J. Mater. Sci.*, 2001, **36**(21), 5227–5230.
16. Shi, Z. M., Pan, F., Liu, D. Y., Liang, K. M. and Gu, S. R., Effects of Ce^{4+}-modified amorphous SiO_2 on phase transformation towards α-cordierite. *Mater. Lett.*, 2002, **57**(2), 409–413.
17. Shi, Z. M., Sintering additives to eliminate interphases in cordierite ceramics. *J. Am. Ceram. Soc.*, 2005, **88**(5), 1297–1301.
18. Orenstein, R. M. and Green, D. J., Thermal shock behavior of open-cell ceramic foams. *J. Am. Ceram. Soc.*, 1992, **75**(7), 1899–1905.
19. Kumar, S., Singh, K. K. and Ramachandrarao, P., Synthesis of cordierite from fly ash and its refractory properties. *J. Mater. Sci. Lett.*, 2000, **19**(14), 1263–1265.
20. Kobayashi, Y., Sumi, K. and Kato, E., Preparation of dense cordierite ceramics from magnesium compounds and kaolinite without additives. *Ceram. Int.*, 2000, **26**(7), 739–743.
21. Montanaro, L., Durability of ceramic filters in the presence of some diesel soot oxidation additives. *Ceram. Int.*, 1999, **25**(5), 437–445.
22. Ervin, G., Oxidation behavior of silicon carbide. *J. Am. Ceram. Soc.*, 1958, **41**(9), 347–352.
23. Jorgensen, P. J., Wadsworth, M. E. and Cutler, I. B., Oxidation of silicon carbide. *J. Am. Ceram. Soc.*, 1959, **42**(12), 613–616.
24. Meek, R. L., Diffusion coefficient for oxygen in vitreous SiO_2. *J. Am. Ceram. Soc.*, 1973, **56**(6), 341–342.
25. Costello, J. A. and Tressler, R. E., Oxidation kinetics of silicon carbide crystals and ceramics. I. In dry oxygen. *J. Am. Ceram. Soc.*, 1986, **69**(9), 674–681.
26. Jacobson, N. S., Corrosion of silicon-based ceramics in combustion environments. *J. Am. Ceram. Soc.*, 1993, **76**(1), 3–28.
27. Shi, Z. M., Liang, K. M. and Gu, S. R., Effects of CeO_2 on phase components and properties of cordierite ceramics. *J. Tsinghua Univ.*, 2001, **41**(10), 1–4.
28. Philipse, A. P. and Schram, H. L., Non-Darcian airflow through ceramics foams. *J. Am. Ceram. Soc.*, 1991, **74**(4), 728–731.
29. Innocentini, M., Pardo, A. and Pandolfelli, V., Influence of air compressibility on the permeability evaluation of refractory castables. *J. Am. Ceram. Soc.*, 2000, **83**(6), 1536–1538.
30. Carman, P. C., *Flow of Gases Through Porous Media*. Butterworths, London, 1956.
31. Rice, R. W., Comparison of stress concentration versus minimum solid area based mechanical property–porosity relations. *J. Mater. Sci.*, 1993, **28**(8), 2187–2190.
32. Rice, R. W., Evaluation and extension of physical property–porosity models based on minimum solid area. *J. Mater. Sci.*, 1996, **31**(1), 102–118.
33. Rice, R. W., Evaluating porosity parameters for porosity–property relations. *J. Am. Ceram. Soc.*, 1993, **76**(7), 1801–1808.
34. She, J. H., Ohji, T. and Deng, Z. Y., Thermal shock behavior of porous silicon carbide ceramics. *J. Am. Ceram. Soc.*, 2002, **85**(8), 2125–2127.
35. Ding, S. Q., Zeng, Y. P. and Jiang, D. L., Thermal shock resistance of in situ reaction bonded porous silicon carbide ceramics. *Mater. Sci. Eng.*, 2006, **A425**(1–2), 326–329.
36. Kingery, W. D., Factors affecting thermal stress resistance of ceramic materials. *J. Am. Ceram. Soc.*, 1959, **38**(1), 3–15.